Cha et al., http://www.jgp.org/cgi/full/jgp.201110611/DC1

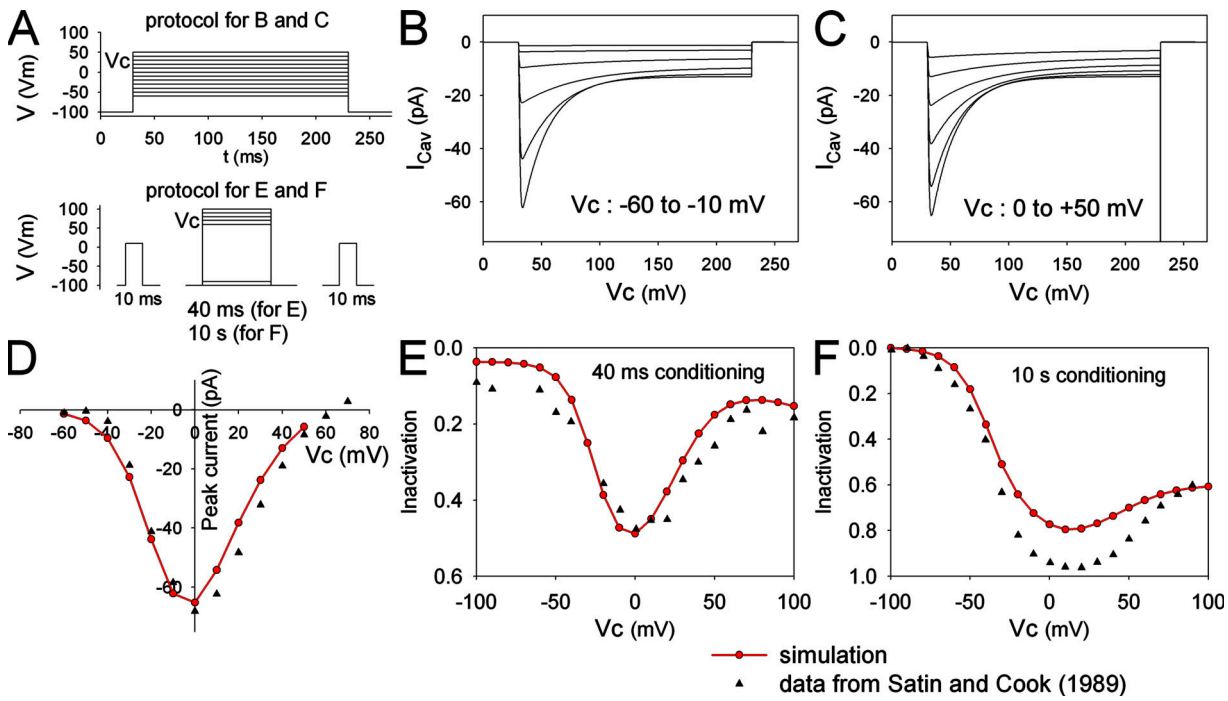

Figure S1. Reconstruction of I_{CaV} in the voltage-clamp experiments of Satin and Cook (1989. *Pflugers Arch.* 414:1–10). (A; top) Voltage-clamp protocol for B and C with 200-ms command pulses (Vc) varying from −60 to +50 mV in 10-mV increments from a holding potential of −100 mV. The lower three-pulse protocol is for E and F. Two 10-ms test pulses to +10 mV were separated by a 40-ms or 10-s conditioning pulse (Vc) ranging from −100 to +100 mV. $[Ca^{2+}]_o$ and [ATP] were 3 and 2 mM, respectively, as used in Satin and Cook. (B and C) Reconstruction of I_{CaV} at test potentials of −60 to −10 mV and 0 to +50 mV, respectively. (D) The peak I_{CaV}–V_m relation in the model (red circles and line) compared with experiment (black triangles, duplicated from Fig. 2 B of Satin and Cook). (E) Measurement of Ca^{2+}-dependent inactivation of I_{CaV} using 40-ms conditioning pulses, as described in A. Inactivation was defined by the ratio of peak currents at the second test pulse and the first pulse, plotted against Vc (simulations, red circles and line; experiments, black triangles). The experimental data of Fig. 3 C of Satin and Cook were scaled to give an average inactivation of 0.45 at +10 mV. Simulations reproduced a U-shaped curve with maximal inactivation at 0 mV, in good agreement with the experiment. The small inactivation at −50 to −100 mV is a result of incomplete recovery during the interval of repeated measurements of inactivation, whereas the greater inactivation at Vc > +70 mV is a result of contamination of ultraslow inactivation (f_{us}). (F) Measurement of inactivation using 10-s conditioning pulses. The experimental data (black triangles) were from Fig. 4 B of Satin and Cook.

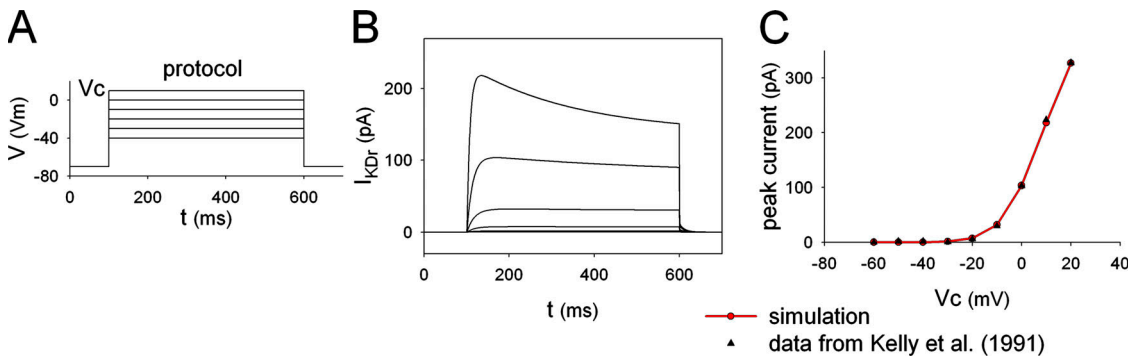

Figure S2. Reconstruction of I_{KDr} in voltage-clamp experiments. (A) Voltage-clamp protocol with 500-ms test pulses (Vc) from −40 to +10 mV in 10-mV increments from a holding potential of −70 mV. (B) Simulated I_{KDr}. The traces are consistent with the experimental records of I_{Kv} current in the presence of Cd^{2+} and paxilline to inhibit a BK current (Houamed et al. 2010. *J. Physiol.* 588:3511–3523). (C) Peak I_{KDr}–V_m relationships from B. The experimental measurements taken from Fig. 1 B of Kelly et al. (1991. *J. Physiol.* 443:175–192) (black triangles) are virtually superimposed with the simulation results (red circles and line).

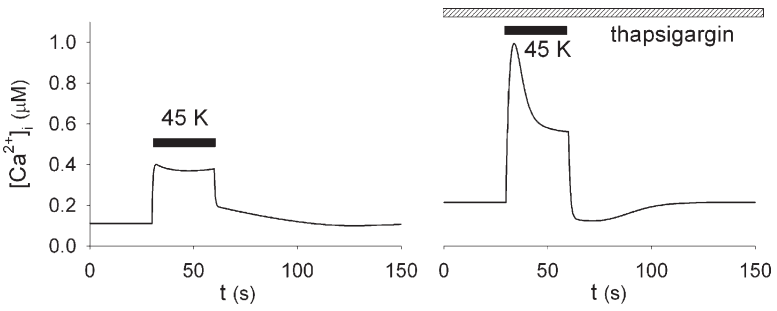

Figure S3. Ca^{2+} transients induced by applying high K^+ pulses before and during the application of thapsigargin. In the presence of 10 mM $[Ca^{2+}]_o$, $[K^+]_o$ was increased for 30 s from the standard 4.5 to 45 mM (horizontal black bars, 45 K, both panels) according to the experimental protocol (Fig. 2 A in Gilon et al. 1999. *J. Biol. Chem.* 274:20197–20205). Blockage of SERCA by thapsigargin (bar with diagonal lines in the right panel) was simulated by reducing P_{SERCA} to 20% of control (from 0.096 to 0.0192 amole ms^{-1}). The open probability of I_{KATP} (G_{KATP}) was set to 1 to simulate the effect of the K_{ATP} channel opener, diazoxide used experimentally, and the amplitude factor of I_{CaV} (P_{CaV}) was reduced by half to reproduce the smaller experimental Ca^{2+} transient.

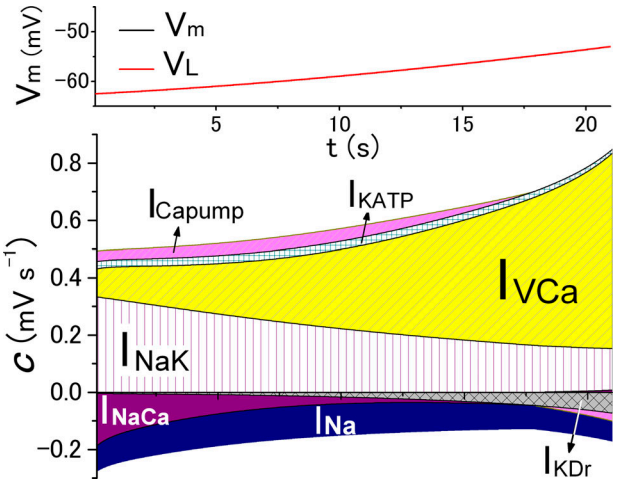

Figure S4. V_L diagram during the interburst period at 8.5 mM [G] determined in the FP model. (Top) Time-dependent changes of V_L (red) and V_m (black), which were virtually superimposed. (Bottom) V_L diagram for c of individual currents indicated by different colors.

Table S1

Initial values of independent variables (X(0))

Independent variables	Initial values
V_m	−48.9045
$[Na^+]_i$	5.80400
$[K^+]_i$	126.776
$[Ca^{2+}]_i$	0.000306139
$[Ca^{2+}]_{ER}$	0.0234849
[ATP]	2.64667
[MgADP]	0.127093
[Re]	0.641950
d_{CaL}	0.101898
U_{CaL}	0.635696
f_{us}	0.827114
r_{KDr}	0.00105694
q_{KDr}	0.970421
m_{Kto}	0.0170783
h_{Kto}	0.301612
$E_{i,tot}$	0.354892
I_1	0.151253
I_2	0.489584

The set of values was obtained when the model shows a steady bursting rhythm at 8 mM [G]. The initial values were used for obtaining all the figures in this paper and Figs. 1, 4, and 5 in our companion paper (Cha et al. 2011. *J. Gen. Physiol.* doi:10.1085/jgp.201110612). These initial values define the present model according to the charge conservation law described in our companion paper.